ORIGINAL ARTICLE

lajss.org© Latin American Journal of Solids and Structures

www.lajss.org

Nonlinear Numerical Evaluation of Dry Precast Beam Column Connection with Embedded Bolts

Srikanth Kallam[a]*, Sanjay. BhanuKumar Borghate[a]

[a]Department of Applied Mechanics, Visvesvaraya National Institute of Technology, Nagpur, 440010, India. E-mails: srikanthkallam.2006@gmail.com, sbborghate@apm.vnit.ac.in

*Corresponding author

https://doi.org/10.1590/1679-78257314

Abstract

Precast dry connected frame systems are faster to construct with less erection efforts. These frame systems are considered non-emulate frame systems. The lateral load behaviour of these connections needs to be evaluated to ensure the desired performance. The performance of these dry connections with embedded bolts proposed was studied by finite elemental analysis. The nonlinear FEM analysis results obtained by considering appropriate elements, and material definition parameters, including failure and interactions, were validated with the experimental results available in the literature. The rigidity of the joints was evaluated using the beamline method. The beamline plot unveils that the joints can be classified as rigid joints. The results reveal that the joints under study have satisfactory stiffness degradation, energy dissipation characteristics, and failure modes like monolithic connection. The numerical procedure developed provide an efficient solution for performance evaluation and seismic design of these precast joints

Keywords

Precast dry joint, Nonlinear finite element analysis, Lateral load response, Seismic performance, Cyclic response

Graphical Abstract

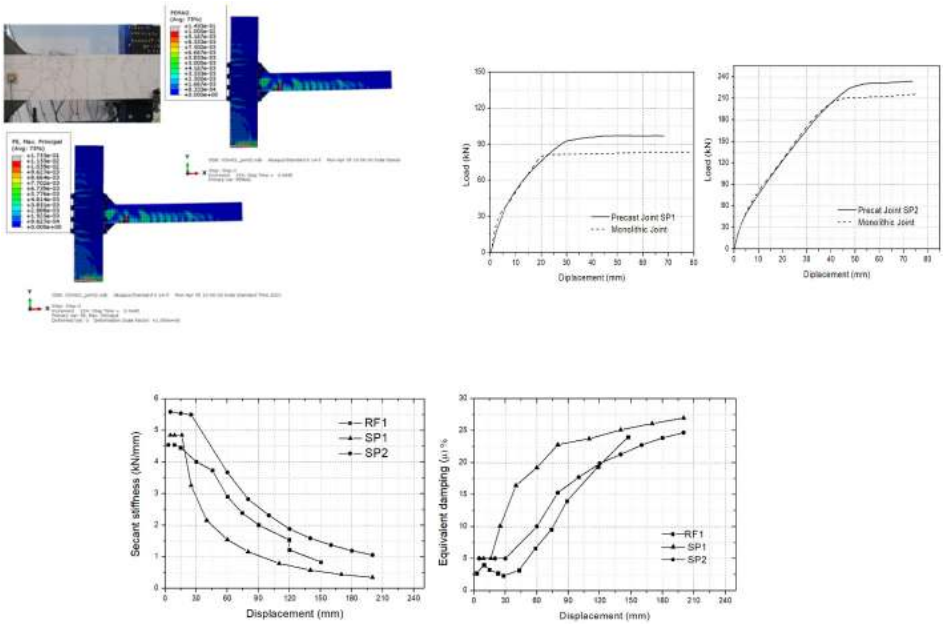

Received: September 30, 2022. In revised form: October 06, 2022. Accepted: October 09, 2022. Available online: October 13, 2022.
https://doi.org/10.1590/1679-78257314

Latin American Journal of Solids and Structures. ISSN 1679-7825. Copyright © 2022. This is an Open Access article distributed under the terms of the Creative Commons Attribution License, which permits unrestricted use, distribution, and reproduction in any medium, provided the original work is properly cited.

1. INTRODUCTION

With the rapid advancement of construction activities, precast construction has witnessed a rise due to its inherent advantages in terms of productivity, economy, and quality control. However, the catastrophic failure of precast structures, particularly the failure of joints during earthquakes, showed a possible drawback in implementing these systems. The research paper by D'Arcy, et al. (2003) has described the sequential development of code provisions for precast concrete structures in the United States. The seismic design provisions for precast concrete structures were first given in ACI 318-02 (2002). These provisions are derived from the recommendations of 2000 NEHRP (FEMA, 2001). According to ACI 318-02 (2002), the precast system shall be designed as emulate monolithic special moment frames, special structural walls or dual frame systems in high seismic regions. Systems like dry jointed non-emulate monolithic and hybrid connection frame systems need to be validated as per the criteria established by ACI T1.1 (2001). The research paper by Park (1995) contains the design and construction aspects of precast concrete structural design that are in practice in New Zealand. The New Zealand code for concrete design, NZS 3101: 1995, contains the provisions for seismic design of precast systems.

Lateral stiffness, strength and ductility are important characteristics to ensure the seismic performance of any structural system. Wet connected systems consist of precast elements connected by cast-in-situ wet joints was widely used precast system in New Zealand and Japan in late 90's. The research by Park (1995) enumerates these wet jointed systems consisting of cast-in-situ columns and precast beams connected with lapped rebars in the joint region, a system with precast beams with grout sleeves to accommodate column rebars, and a system with precast T- units connected one over other through precast columns with a grouted sleeve to form a precast structural system. The effectiveness of these emulate monolithic systems, their constructability and analytical modelling issues were studied by Park (1995), Nishiyama (1990) and Otani (1981). Precast wet joint consists of U-shaped shell at the end of precast beam element to act as permanent formwork for wet concreting in the joint region has been investigated by Parastesh et al. (2014), Khaloo and Parastesh (2003). The experimental studies on these joints revealed that the seismic performance of this joint emulates monolithic behaviour.

Precast dry mechanical connection system (Kulkarni et al. 2008; Nzabonimpa et al. 2017; Aninthaneni et al. 2018; Vidjeapriya and Jaya 2013) consist of steel inserts, bolts, welding, anchors are faster to construct with less erection efforts. Dry mechanical connections transfer load from beam to the column through steel inserts or bolts embedded in the column; hence, the load transfer mechanism differs from the monolithic connection. These connections are treated as non-emulative monolithic connections. A detailed experimental or numerical study as per the acceptable criteria (ACI T1.1 2001) is required to study the seismic performance of these connections. Hybrid systems consist of unbonded post-tensioned tendons (UPT) at centre of the beam and locally deboned rebars to act as energy dissipator is another kind of non-emulate monolithic precast post-tensioned structural system. These precast post-tensioned systems consist of beam and column elements designed for strength, and nonlinear deformations can occur at the connection interface by gap opening (Priestley et al. 1999; Gavridou et al. 2017; Hawileh et al. 2010; Rahman and Sritharan 2007).

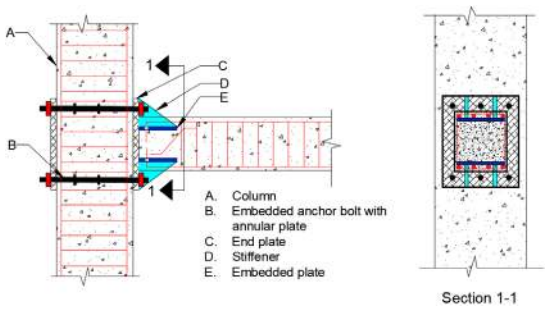

Figure 1. Layout of the connection

Precast structures with Dry mechanical connections are faster to construct. But since the connections are non-emulative monolithic connections, a detailed study is required to ensure seismic performance. Vidjeapriya and Jaya (2013) made an experimental study on precast beam column connection consisting of corbel, cleat angle with single stiffener, and cleat with double stiffener. According to this research, dry connections the ultimate load-carrying capacity of the dry connections is lesser when compared to monolithic connections. Steel billet connections are also the dry connections. This connection consists of a steel box section embedded in the column that acts as a corbel (hidden inside the beam) to transfer shear and moment to the column. Elliot et al. (2003) have conducted an experimental study on corbel connections. The research revealed that billet connections are semi-rigid connections. The research proposed equations to calculate the percentage rigidity of connections and effective length factor of columns in semi-rigid sway frames.

Aninthaneni et al. (2018) conducted an experimental investigation on the performance of demountable beam end plate connections. The cyclic response obtained by the experimental study on endplate connection has been compared with the

response of the wet jointed system. The cyclic response and other connection characteristics are comparable with the monolithic connection. Experimental investigation on dry connections by Choi (2013) has revealed that connections designed to form plastic hinge location away from the joint face possess better energy dissipation capacity and ductility, while connections designed to form plastic hinge right at the face of the joint has characteristics like monolithic beam-column joint.

Nzabonimpa et al. (2017) made a nonlinear finite element study on dry end plate connection with steel inserts embedded inside concrete for exterior beam-column joints. The finite element model has been calibrated with experimental results and made studies on strength, stiffness degradation characteristics and failure modes using the calibrated FEM model. The analytical results have complied with the experimental results. Bahrami et al. (2017) has performed nonlinear FEM analysis on steel billet connections. For this study, the FEM model was developed for the internal joint using 3D solid elements; concrete material was defined with concrete damage plasticity (CDP) criteria for yielding. Contacts were defined using the contact definition capability available in ABAQUS. Kulkarni et al. (2008) performed a nonlinear analysis on hybrid beam-column connections. The joint was modelled using 2D plane stress elements in DIANA software.

The dry connections investigated, consist of steel billets (Elliot et al. 2003), corbel with stiffeners (Vidjeapriya and Jaya 2013), end plate with steel inserts (Nzabonimpa et al. 2017), end plate with embedded plate and stiffeners (Aninthaneni et al. 2018) were the major studies on dry joints. The joint with endplate, embedded plate, and stiffeners (Aninthaneni et al. 2018) is easy to erect/construct and remove/replace the components. But the joint (Aninthaneni et al. 2018) with bolt in sleeve requires large number of bolts and makes it difficult to adopt these kinds of joints. Hence the joint is modified with embedded bolts. The systemic arrangement of the connection is in Figure 1. The seismic performance of this joint (Figure 1) was investigated numerically as .part of this present study. Joint characteristics have an important role in the lateral load behaviour and seismic performance of a precast framed structure. In the present study, FEM analysis was performed on beam-column external joints that are designed following the capacity design principles. Columns and beams are designed to satisfy strong column-weak beam phenomena; components of connections like endplate, bolts and embedded plats are designed to remain elastic, allowing plastic deformations to occur in the beam by flexure. These dry end plate connections are designed considering the equivalent yielding line of all the possible failure modes as per EN 1993-1-8. The Finite element study that is conducted in ABAQUS software on this beam-column joint is (i) To check the elastic stiffness of the joint when compared to the monolithic joint (ii) To obtain the force-displacement response of the joint and yield point (iii) To obtain stiffness degradation of the joint (v) To study the semirigid behaviour (vi) To observe the failure mechanism.

2. DESCRIPTION OF THE PRESENT STUDY

The dry joint proposed consists of beam-column elements connected by end plates, embedded plates, stiffeners, and bolts to transfer the moment and shear from beam to column by tension in bolts and by bearing pressure from the endplate. The schematic arrangement of the connection is shown in Figure 1. As in the figure, the endplate is welded to two embedded plates and two stiffeners embedded in beam concrete and bolted to the column. The longitudinal steel bars are anchored by passing the rebars through the slotted holes in embedded plate. Stiffeners, which are triangular-shaped plates welded to the horizontal embedded plate and to the endplate, as in Figure 1, increases the connections moment capacity and offer rotational stiffness. The anchor bolts with annular plate embedded in column distributes the tensile force in the bolts to the joint region.

Structures designed shall possess adequate ductility, energy dissipation and lateral stiffness characteristics to ensure seismic performance. IS 13920-2016 provides the capacity design considerations for the design of monolithic concrete structures. But the load transfer mechanism and post elastic behaviour of the precast structure varies from monolithic structure (Kulkarni et al. 2008; Nzabonimpa et al. 2017; Aninthaneni et al. 2018; Vidjeapriya and Jaya 2013). Table 1 provides these major capacity design considerations and their applicability to a dry mechanical precast structure.

Table 1. Ductile design considerations for precast framed structure.

Design acceptance criteria	Dry mechanical framed structure
Shear capacity of beam	Design shear will be the maximum shear considering all possible failure mechanism (provisions of section 6.3.3 of IS 13920-2016 were utilized to meet the criteria)
Shear capacity of column	As like beam, design shear will be the critical force considering all possible failure mechanism (provisions of section 7.5 of IS 13920-2016 were utilized to meet the criteria)
Beam to column capacity ratio	Moment carrying capacity of the column meeting at the joint should be higher than the capacity of the beam to ensure strong column weak beam phenomena (provisions of section 7.2 of IS 13920-2016. were utilized to meet the criteria)
Anchorage of reinforcement	Numerical or experimental verification of anchorage of the beam longitudinal bars is necessary
Joint shear	Experimental or numerical verification of the load transfer mechanism is necessary to avoid brittle joint shear failure

Considering the above-mentioned seismic design requirements, a three-story building consisting of 3 bays in X-direction and 4 bays in the Y-direction with 5m bay length and a five-story building with 6m bay spacing was designed. These buildings were designed for seismic zone V with an importance factor 1 as per IS 1893-2016. Like monolithic structures, the elastic analysis was performed considering the effective moment of inertia as per code and considering joints as rigidly connected. The analytical model can predict the distribution of member forces under design level loading with reasonable accuracy.

Two external joints, SP1 and SP2, were chosen for the numerical study from these designed framed buildings. Specimen SP1 was taken from the 3-story building with 5m bay spacing, and specimen SP2 is from the 5-story building with 6m bay spacing. The specimen investigated experimentally (Aninthaneni et al. 2018) was chosen as reference specimen RF1 to validate the FEM results obtained. The specimens SP1 and SP2 were modelled with embedded bolts whereas the experimental specimen, RF1 is modelled with bolts in sleeves as described in section 4.

3. JOINT DESIGN CRITERIA AND DETAILS OF THE CONNECTION

To ensure ductility of the precast buildings, the capacity design considerations stated in Table 1 are considered in the design of precast elements. Following the design considerations, the precast framed building (3 story, 5 story) was designed to ensure ductile failure like monolithic building. The beams in the first floor and second floor of the building will have larger moment demand when compared to the beams at top floor hence the joints in the first and second floor of the building will be critical in terms of shear and capacity ratio. The representative specimens SP1 and SP2 chosen are the external joints stiffensselected from the first/second floor of the precast frame designed. Table 2 provides the moment capacity of beam and column and the capacity ratio (M_{col}/M_{beam}) of all the specimens chosen for study.

The reinforcement details of beams and columns and endplate assembly details for all three specimens are provided in Figure 2. The specimen dimensions are also mentioned in the figure. These specimens represent approximately half the bay length and story height of the designed building.

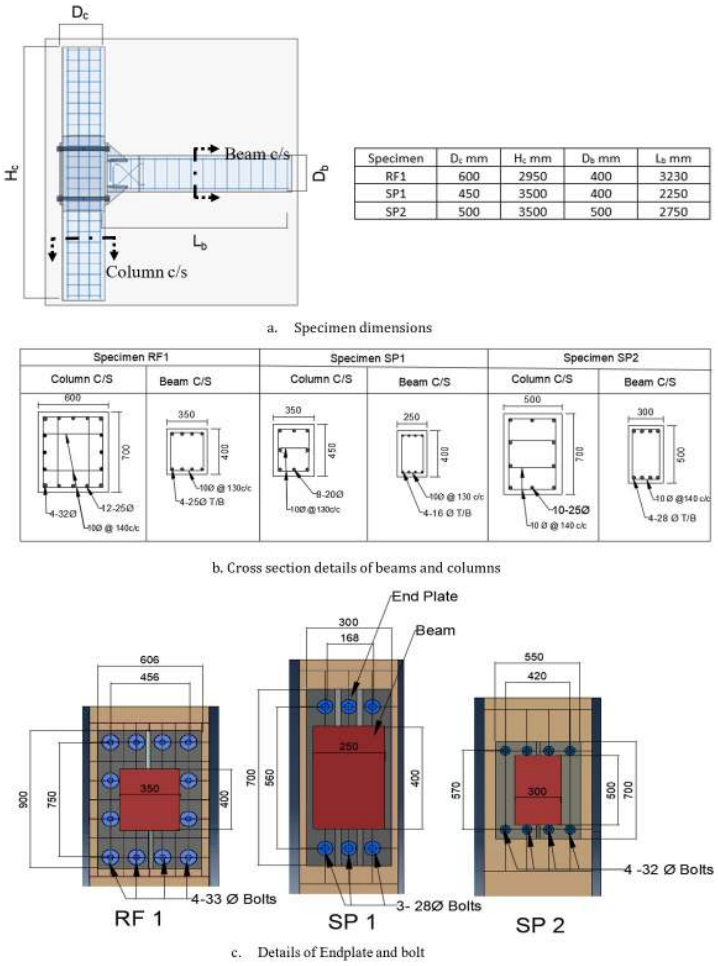

Figure 2. Beam column joints considered for study.

Table 2. Capacity ratio of the joints considered.

Joint	Column Size mm	Beam Size mm	Column Capacity M_{col} kNm	Beam Capacity		M_{col}/M_{beam} Capacity Ratio
				M_{hogg} kNm	M_{sagg} kNm	
RF1	C 600 X 700	B 350 X 400	907	309	309	4.65
SP1	C350x450	B250x400	175.43	96.27	96.27	3.64
SP2	C700x500	B300x500	490	387	387	2.53

Table 3. Details of connections designed and the reference specimen

Specimen	Column dimensions (mm)	Beam dimensions (mm)	End plate size (mm)	Embedded plate	Stiffener plate	Bolt T/B
RF1	C 700 X 600	B 350 X 400	PL 900 X 606 X 25	PL 25 mm thk	PL 20 mm thk	5 nos 33 mm Ø
SP1	C 450 X 350	B 250 X 400	PL 300 X 700 X 25	PL 20 mm thk	PL 20 mm thk	3 nos 28 mm Ø
SP2	C 700 X 500	B 300 X 500	PL 700 X 550 X 40	PL 20 mm thk	PL 20 mm thk	4 nos 32 mm Ø

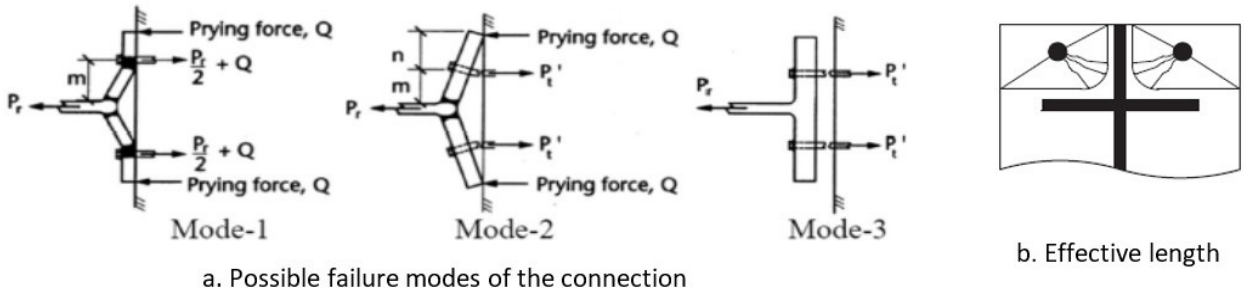

Figure 3. End plate connection design – Failure modes and Effective length (EN 1993-1-8)

Connection components like endplate, bolts and embedded plate are designed to remain elastic, considering the beam capacity- shear and ultimate moment capacity. The endplate was designed considering all possible failure modes (Figure 3) such as (i) mode-1 Yielding of the plate, (ii) Mode-2: simultaneous yielding of the plate and bolts failure (iii) Mode-3: bolts failure. The moment capacity of the endplate is obtained by converting the mentioned yielding pattern into an equivalent yielding line length as per the criteria provided by EN 1993-1-8. Table 3 provides the detail of endplate connection for specimen SP1 and SP2 designed, considering these criteria.

4. FINITE ELEMENT MODELLING OF THE JOINT

Three-dimensional finite elemental models of the joins had been developed in ABAQUS. Nonlinear FEM analysis was performed on the developed model to study the seismic performance. The stress-strain relationship of the material, the numerical representation of the material, including damage criteria and selection of damage parameters, element selection and element meshing, boundary conditions, the definition of interaction surfaces and solution methodology are discussed in detail in this section.

4.1. Concrete material model

The behaviour of reinforced concrete is complex because of the presence of steel and concrete. Concrete behaviour is brittle, whereas steel behaviour is ductile. Therefore, the damage models can describe the concrete behaviour, whereas steel behaviour can be described using plasticity models. Since steel is ductile, the behaviour of reinforced concrete can be simulated using models that combine plasticity and damage. These models are well suited for representing failure modes that are based on compression crushing and tensile cracking. This paper uses the concrete damage plasticity model proposed by Alfarah et al. (2017) to model the reinforced concrete material. The advantage of this approach is that the result variation is less dependent on the mesh size chosen, and the output is less sensitive to material definition parameters. Hence accurate calibration of material definition parameters is not required (Alfarah et al. 2017)

The stress-strain relation of concrete in tension and compression and damage parameters required to define the material can be observed from Figure. 4a and b. The figure illustrates the unloading and reloading branches of the stress-strain curve and defines the damage-plasticity behaviour. The descending branches of the curve were generated to ensure nearly mesh-independency. In the figure, f_{ck} and ft represents mean compressive and mean tensile strength,

respectively, and the corresponding strains are ε_{ck} and ε_t, respectively. The first segment of the stress-strain curve is linear, with $\sigma_{c(1)} = E_0\ \varepsilon_c$ The second (ascending) segment is quadratic (equation 1).

$$\sigma_{c(2)} = \frac{E_c\frac{\varepsilon_c}{f_{ck}} - \left(\frac{\varepsilon_c}{\varepsilon_{ck}}\right)^2}{1+\left(E_c\frac{\varepsilon_{ck}}{f_{ck}} - 2\right)\frac{\varepsilon_c}{\varepsilon_{ck}}}\ f_{ck} \tag{1}$$

In the above equation (1), E_c is the modulus of elasticity of concrete for zero stress, given by $E_0/\left(0.8 + \frac{0.2f_c}{88}\right)$, were $E_0 = 5000\sqrt{f_{ck}}$.The expression for the third (descending) segment is given by

$$\sigma_{c(3)} = \left(\frac{2+\gamma_c f_{ck}\varepsilon_{ck}}{2f_{ck}} - \gamma_c\varepsilon_c + \frac{{\varepsilon_c}^2\gamma_c}{2\varepsilon_{ck}}\right)^{-1} \tag{2}$$

In the above expression γ_c is the non-dimensional parameter to consider the effect of the element size. The mean tensile strength of concrete was considered as $f_t = 0.7\sqrt{f_{ck}}$ (Figure 4b). The descending branch of the tensile stress-strain curve was also considered as per the formula suggested by Alfarah et al. (2017), as a function of crack width and critical crack opening and fracture energy.

Damage in the damage plasticity model is correlated with the failure mechanisms consisting of concrete crushing and cracking; therefore, damage reduces elastic stiffness. According to scalar-damage theory, the isotropic stiffness degradation is defined by a degradation parameter "d". Damage is defined in compressive and tensile states "dc" and "dt" as functions of plastic strains. Damage parameter (dc or dt) takes values ranging from zero (for undamaged material) to one (for fully damaged material). The damage parameters dt and dc for the RC material has been calculated based on the procedure described by Alfarah et al. (2017).

The flow rule related to concrete damage plasticity was established in the model as a critical element of plasticity theory, using non-associated flow potential function $G(\sigma)$. The Drucker- Prager hyperbolic function was utilised in the model as a non-associated flow potential function as in Equation.3.

$$G(\sigma) = \sqrt{(\epsilon\sigma_{to}\tan\psi)^2 + \bar{q}^2} - \bar{p}\tan\emptyset \tag{3}$$

Table 4. Concrete damage plasticity parameters

Parameter	ψ	K_C	$\frac{f_{bo}}{f_{co}}$	ϵ
Value Considered	36°	0.67	1.16	0.1

The equation involves material parameters. The first parameter is dilation angle ψ which is a concrete performance characterising parameter when subjected to triaxial compound stress state. The value ψ typically varies from 32^0-46^0. The next parameter ∈ is eccentricity, which adjusts the shape of the hyperbola in the plastic potential flow function. The default value of the eccentricity parameter is equal to 0.1. The third parameter to define material is Kc, which is the ratio between deviatoric stress magnitude in uniaxial tension and compression. The default value of Kc is equal to 0.67. Another material parameter, stress ratio f_{bo}/f_{co} has a negligible effect on material behaviour, and it can be considered as 1.16 by default. Table 4 provides the values of these parameters considered for FEM analysis.

4.2. Steel material model

A multi-linear kinematic hardening model was used for all structural steel elements in both tension and compression. In this model, the stress-strain relation of steel was considered bi-linear. The elastic and plastic options available in ABAQUS were used to define the elastic and post-yield behaviour of the material. The plastic material definition option available in software considers von Mises yield criterion to define isotropic strain hardening and softening behaviour of the material. The modulus of elasticity, Poisson's ratio and density of all steel elements were assumed to be 200 GPa and 0.3, 7800 kg/m^3, respectively. The idealised stress-strain behaviour of steel material used for the FE modelling is in Figure 5. Properties of these materials were also stated in Table 5.

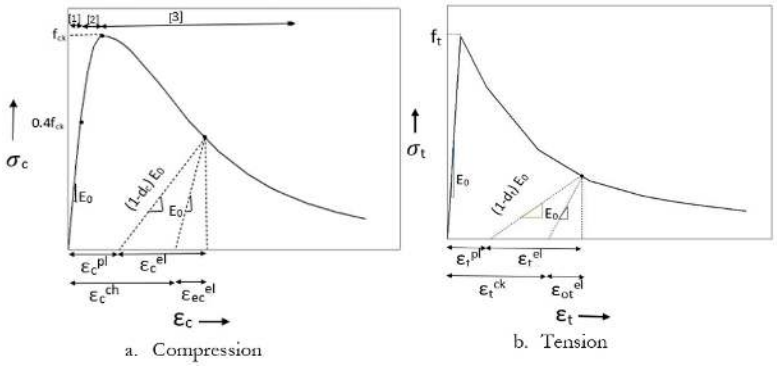

Figure 4. Concrete material parameters (CDP)

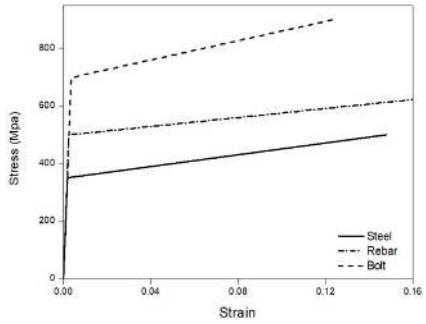

Figure 5. Idealised stress strain curve for steel material

Table 5. Material properties considered for the study

Material Property	Strength Mpa
Compressive strength of concrete fck	40
Yield strength of steel fy	350
Ultimate strength of steel fu	480
Yield strength of rebar fy	500
Ultimate strength of rebar fu	625
Yield strength of bolt (grade – 8.8) fy	700
Ultimate strength of bolt (grade – 8.8) fu	900

4.3. Element properties and meshing

The components of connection like concrete, steel plates and bolts were modelled as three-dimensional (3D) elements while reinforcing bars were modelled as truss elements. An 8 nodal brick element titled C3D8R available in ABAQUS was used to model all the connection components except rebars. The solid element with reduced integration has three degrees of freedom at each node. This element with hourglass control capability available in the software simulates the behaviour with reasonable accuracy while being computationally efficient. The rebar was modelled as 3D truss elements denoted as T3D2 in ABAQUS software. Rebar can be included in the model by embedding rebar into the continuum. Hence, rebars were modelled by truss elements, and the embedded capability in the software takes care of the interaction between bars and concrete. This option interpolates the node related to the concrete element with the node related to the rebar. This embedded option can simulate the interaction between concrete and rebar to an acceptable accuracy (Najafgholipour and Arabi, 2019).

Specimen RF1, SP1 and SP2 consist of 94802, 39820 and 65841 elements respectively. All the parts were meshed by the appropriate meshing algorithm available in ABAQUS to obtain well-shaped elements and achieve convergence. A finer mesh is assigned in areas of importance and at locations where stress concentration is expected to occur, and the coarse mesh was used in other locations. Critical components of connection such as end plates, bolts, and stiffener plates were assigned with finer mesh to obtain accurate numerical results.

4.4. Loading and boundary conditions

The exterior beam-column specimens under study were applied with the required displacement to study the performance. The reference specimen RF1 was analysed considering boundary conditions and loading, similar to the

experimental specimen (Aninthaneni et al. 2018), to validate the results. The specimen SP2, the external joint in the building with 6m bay spacing like the reference specimen, was considered pinned at the bottom. Beam end was considered with roller support, allowing horizontal displacement. The top of the column was applied with a monotonic displacement load in a horizontal direction (Aninthaneni et al. 2018; Ertas et al., 2006). Whereas specimen SP1, the external joint in a building with 5m bay spacing, was considered pinned at the bottom and top of the column. Beam tip was considered free, and it was applied with a monotonic displacement load (Aninthaneni et al. 2018; Vidjeapriya and Jaya 2013). The boundary conditions and loading considered is illustrated in Figure 6. Both the boundary conditions have a similar effect and are suitable to study the joint characteristics. Axial load on the column has a considerable effect on lateral elastic stiffness and strength of the joint (Bahrami et al. 2017). The columns were applied with a constant axial load (for all the specimens) in step 1 before applying displacement. The load equal to 10% of the compressive strength of concrete was applied as uniform pressure on top of the column. The specimens are symmetric about the z-axis; taking advantage of symmetry, computational time can be reduced by applying symmetric boundary in the z-direction (Krolo et al., 2016; Shaheen et al., 2017). The symmetry boundary condition applied reduces the number of elements by half.

4.5. Modelling of contact elements

The performance characteristics of connection depend on the interaction between the components and the load distribution between the elements. Hence interaction properties defined is important to simulate the actual behaviour. The surface-to-surface contact definition procedure in software was employed in this study to define the contact properties between the elements. Surface- surface contact assignment procedure requires two surfaces in contact, this procedure of assignment has reliable results compared to the node to surface contact assignment. Out of the two surfaces in contact, one surface was assigned as master surface, and the second was assigned as slave surface. Master surface was assigned with coarser mesh when compared to the slave surface. The surface-to-surface contacts are defined in ABAQUS through tangential and normal behaviour. Tangential behaviour was assigned with a friction coefficient of 0.45 for the contact between steel and concrete and 0.3 for steel-to-steel contact, while normal behaviour was defined as hard contact.

Forces and stress from the embedded plate endplate transfer to the column through bolts. Hence bolts and endplates have a critical role in transferring the forces and ensuring the connection performance. All the major contacts defined are illustrated in Figure 7. Like the rebars, embedded plates and bolts were assigned with embedded contact definitions for specimens SP1 and SP2. Whereas bolts in sleeves of RF1 are assigned with surface-to-surface contact definition parameters. Pre-tension force was applied for bolts in sleeves of specimen RF1 to ensure firm contact between column face and endplate and to avoid bearing failure of the plate. Bolts pre-tension was applied as bolt load in ABAQUS by splitting the bolt shank and applying a magnitude of preload force on two parallel surfaces in the bolt shank. The welded connection between the embedded plate and endplate, endplate and stiffener, stiffener and endplate were applied with tie constraint in ABAQUS.

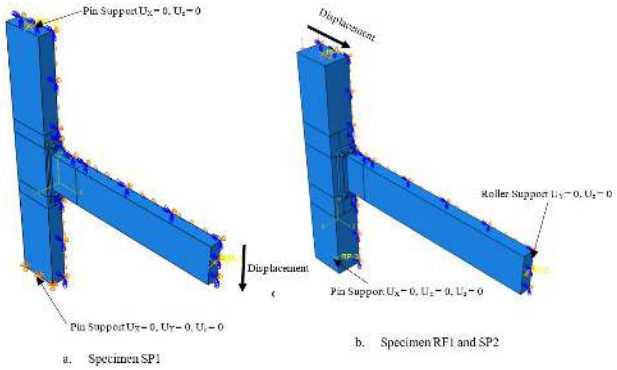

Figure 6. Boundary conditions and loading

4.6. Solution methodology

Nonlinear Finite elemental analysis was performed on the specimens to study the performance of these dry mechanical connections. The specimens under quasi- static loading were studied using the static general algorithm available in ABAQUS. The static general method is an iterative method. The entire step is divided into a series of smaller intervals in this method, which is most suitable for solving nonlinear static problems. The analysis of bolts in sleeve is performed in four steps; column axial load was applied in step1, bolt load was applied in step 2. In step 3, bolts are fixed at the current length. The required quasi-static displacement load was applied in the last step of the analysis. Whereas

the analysis of models with embedded bolts are performed in two steps. Column axial load is applied in Step 1 and displacement load is applied in the second step of the analysis.

5. RESULT OF FEM ANALYSIS

Three-dimensional nonlinear analysis using ABAQUS static general algorithm was performed on the specimens, considering the boundary conditions, and loading as described in the previous section. The force-displacement response obtained provides input such as joint elastic stiffness for analytical modelling of the precast building. Also, the response provides information regarding the yield point required for nonlinear modelling of the precast building. A beam-column joint designed, following strong column weak beam phenomena and beam and column capacity shear, have three possible failure modes. The mode of failure may be beam failure in flexure or joint shear failure or by both (Najafgholipour and Arabi, 2019). The failure mode was observed as part of the FEM analysis.

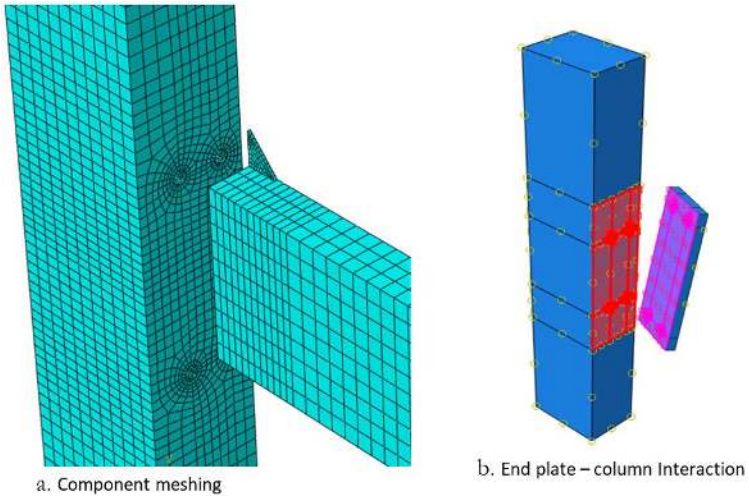

Figure 7. Component meshing and interactions defined

5.1. Verification of finite element model

The reference specimen RF1, which is same as experimental specimen (Aninthaneni et al. 2018) with respect to geometry, boundary conditions were analysed for monotonic load response. A three-dimensional nonlinear analysis was performed on beam-column joints modelled with endplate, embedded plates, stiffeners, and bolts. Plates embedded in beam concrete transfer the forces from beam to endplate. The Stiffeners modelled with tie connection to the endplate and embedded plate increases the rotational stiffness of the joint so that the endplate connection remain elastic while the beam reaches its ultimate moment capacity (plastic moment capacity). The results of the FEM analysis were compared with the experimental data and also with its monolithic counterpart. The load-displacement response of the specimen and the corresponding experimental results can be observed in Figure 8. Figure 9 provides the failure mode, plastic deformations in the critical region, and the corresponding crack pattern of the experimental specimen at 3 percent drift level.

The force-displacement response of the specimen RF1 (Figure 8) obtained numerically matches experimental results with reasonable accuracy as the difference is 4% or less. The plot reveals that the connection initial stiffness and yield point of the connection is comparable with experimental results. The FEM plot captured the yield point and also the ultimate point. The results are sufficient to obtain the linear and nonlinear behaviour of the. joint. Considering the computational time required for nonlinear material like concrete the strain-softening behaviour like the experimental plot and also the cyclic response was obtained through the analytical modelling as described in section 6. In a concrete damage plasticity model, cracks can be graphically represented by introducing an effective crack direction, and the direction of the maximum principal plastic strain, as it is normal to the crack plane, determines the crack direction (Earij et al., 2017). Lubliner et al. (1989) assume that cracks are initiated at points where the tensile equivalent plastic strain and the maximum principal plastic strain are both positive. Therefore, the contour plots of the maximum principal plastic strain (PE, Max, Principle), shown in Figure 9, simulate the crack initiation and propagation at critical sections during loading. Like PE, Max, principal the plot PEMAG, a scalar variable, represents the material inelastic deformations (Earij et al., 2017). If this variable is greater than zero, the material has crossed its yielding limit. Those parts of the lug that have yielded can be identified in a contour plot of PEMAG. The contour plots of FEM analysis in Figure 9 represent the cracking pattern and plastic deformation in the critical region. The cracking pattern obtained from ABAQUS analysis

is compared with the experimental results (Aninthaneni et al. 2018). The location and the cracking pattern for the finite element model and the experimental beam are nearly the same. From the contour plot, it is conclusive that the joint failure is by yielding of beam rebar near the face of the joint while the connection components and joint remain elastic, which is the desirable mode of failure as like monolithic behaviour. The comparison of numerical results with the experimental results shows that the FEM model could capture the overall behaviour of the connection up to the ultimate point with reasonable accuracy.

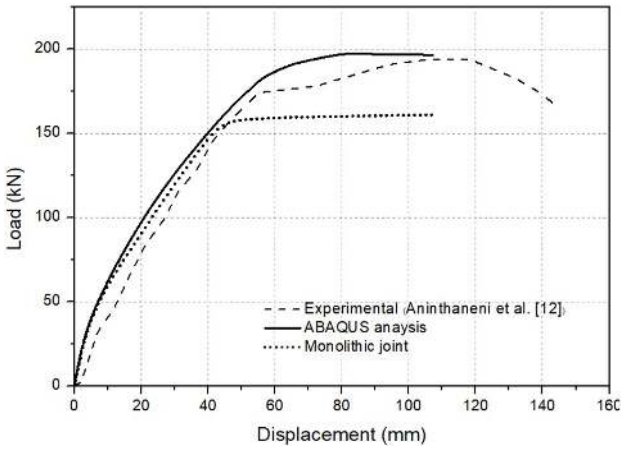

Figure 8. Load-displacement response of specimen RF1

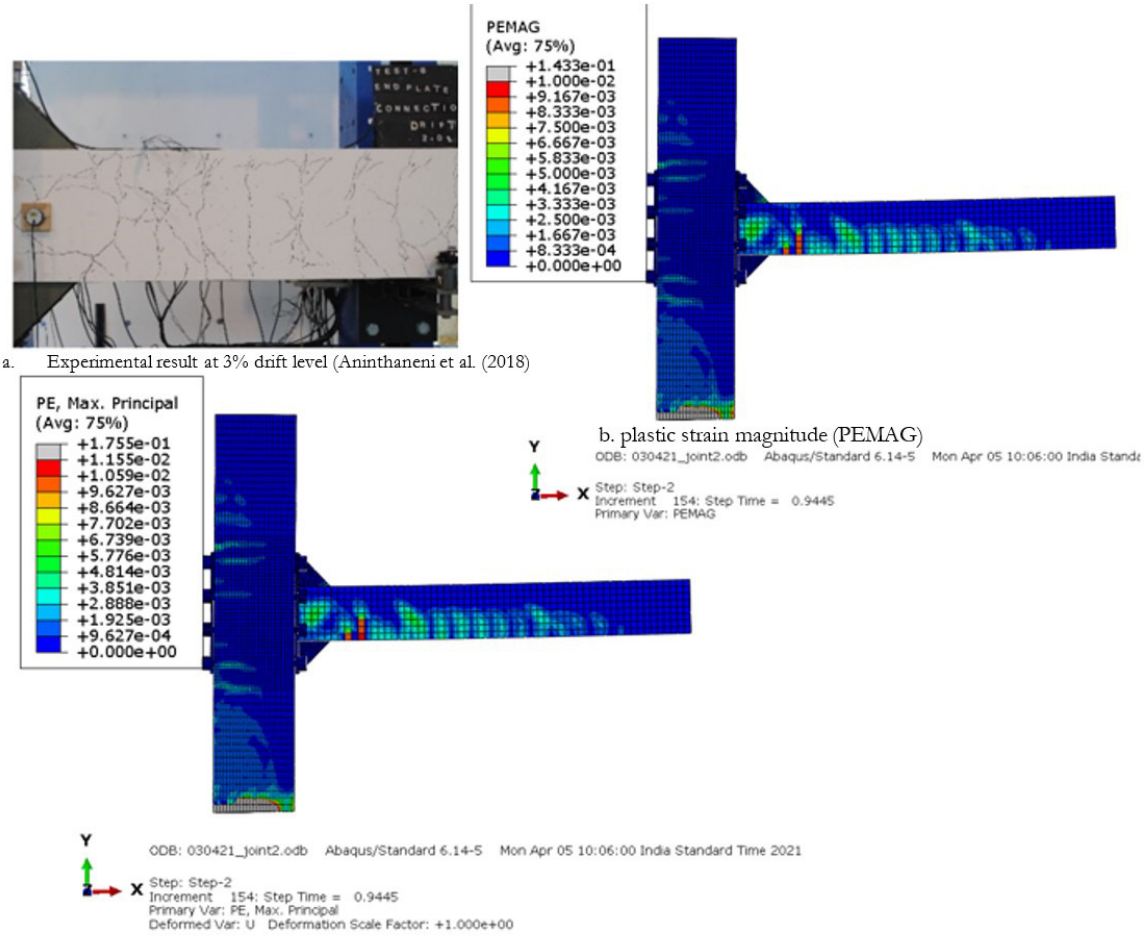

a. Experimental result at 3% drift level (Aninthaneni et al. (2018)

b. plastic strain magnitude (PEMAG)

c. Plastic deformations and Cracking pattern of the reference specimen RF1 (PE max principal)

Figure 9. Validation of FEM results of reference specimen RF1

5.2. Study on capacity of joints with bolt-in sleeves and joints with embedded bolts

The joints with bolt and sleeve will have excessive elongation under tensile loads. The effect of bolt elongation and numerical modelling technics were studied by Krolo et al. (2016). The elongation will contribute to the joint deformations and relative rotations in the joint region. This results in reduction in capacity of the joint. Such a semirigid behaviour due to relative rotation of the joints were studied by Elliot et al. (2003), Elliott and Jolly (2013). Though the bolts are safe to carry the tensile load, the excessive deformations will contribute to reducing the capacity. To avoid excessive deformations, a large number of bolts are necessary; otherwise, it is preferable to have embedded bolts instead of bolts in sleeve.

To illustrate the effect of excessive elongation, a numerical study was performed considering the connections with bolt-in-sleeve and embedded bolts. The study was made on RF1, SP1 and SP2. The obtained force-displacement response of the joints is in Figure 10. The response illustrates the effect of bolt elongation on the characteristics of the connection.

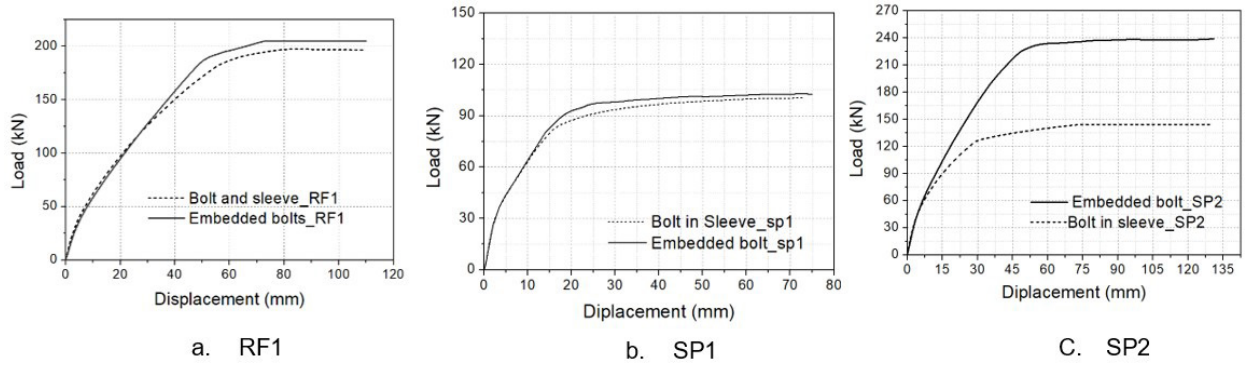

Figure 10. Force-displacement response of the joints with bolt-in-sleeve and with embedded bolts

As in Figure 10, the reference specimen RF1 and specimen SP1 have a negligible effect of bolt elongation, whereas specimen SP2 exhibits a considerable reduction in connection capacity due to excessive bolt elongation. The deformation due to elongation can be observed in Figure 11. The study concludes that the effect of bolt elongation on joint characteristics depends on bolt arrangement, number and diameter of the bolts, and relative size and capacity of the members. To avoid the effect of bolt elongation, the bolts are modified as embedded bolts with an annular plate instead of the bolt-in-sleeve for further study. The annular plate will transfer the stress safely to the concrete core region over a larger area.

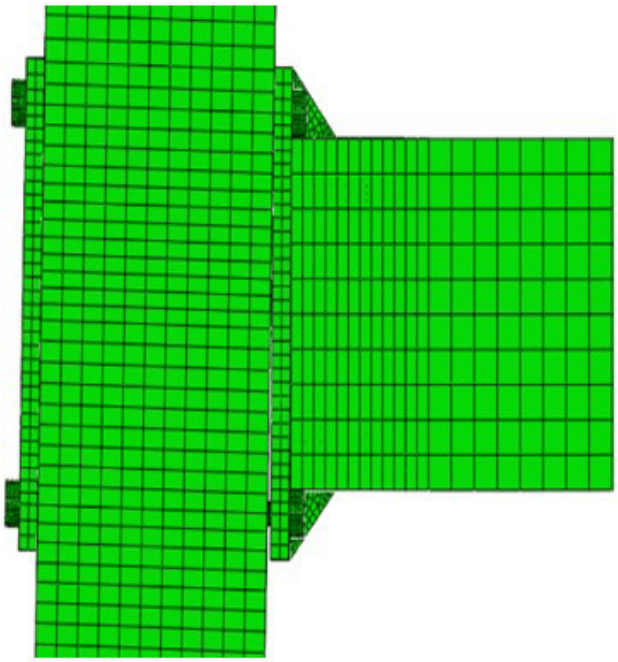

Figure 11. Relative rotation of the joint SP2 due to excessive elongation of the bolt

5.3. Results of FEM analysis – Specimen SP1 and SP2

The precast joints SP1 and SP2 that are designed to ensure ductile failure were also analysed numerically to study the joint characteristics. Force displacement response and stress contours obtained from the analysis are in Figure 12, Figure 13 and Figure 14. Obtained results are compared with the corresponding monolithic joint response results to track the joint elastic and inelastic behaviour. Figure 12 provides the force-displacement response of the specimen SP1 and SP2. Figure 13 and Figure 14 provide the plastic deformation PE (max, principle) and the plastic strain magnitude PEMAG, which are scalar measures of the accumulated plastic strain and Mises stress in rebars of SP1 and SP2 joints, respectively.

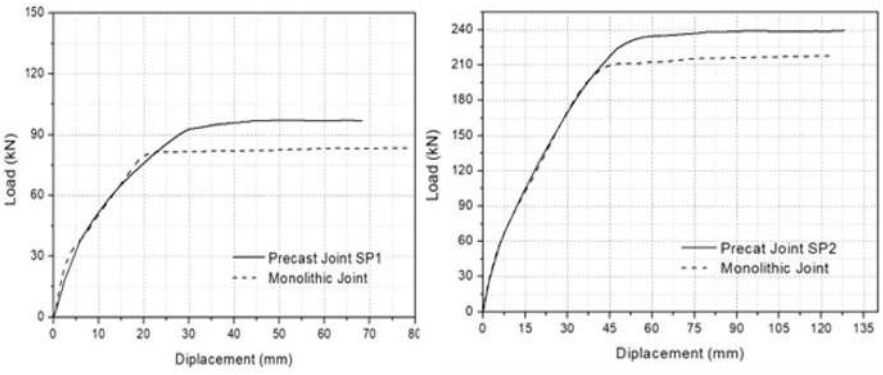

a. Specimen SP1 b. Specimen SP2

Figure 12. Force – displacement response of specimen SP1 and SP2

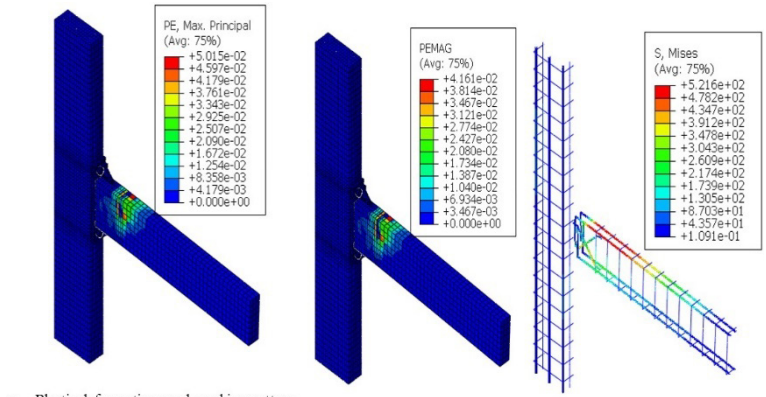

a. Plastic deformations and cracking pattern (PE max principal) b. plastic strain magnitude (PEMAG) c. Mises stress in rebar

Figure 13. Finite elemental analysis results of specimen SP1

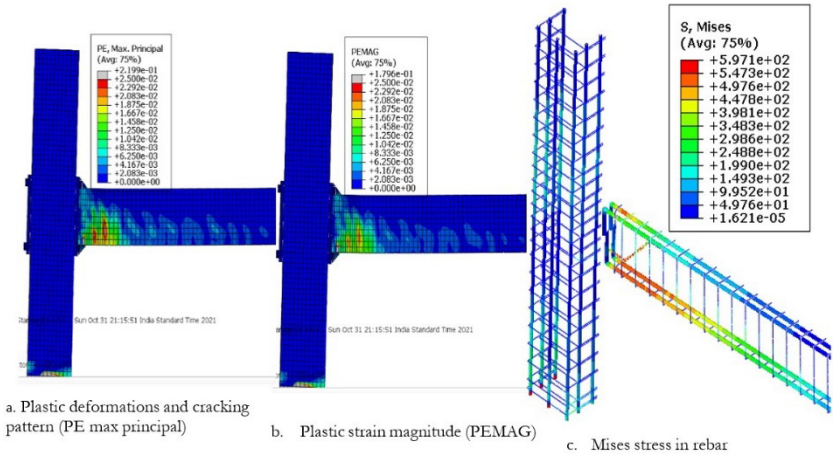

a. Plastic deformations and cracking pattern (PE max principal) b. Plastic strain magnitude (PEMAG) c. Mises stress in rebar

Figure 14. Finite elemental analysis results of specimen SP2

The Force displacement response of both the joints (Figure 12) reveals initial stiffness of the joint is similar to the corresponding monolithic joint, whereas the yielding load and ultimate load of all the joints, including reference specimen RF1 (figure 8), is higher than the monolithic counterpart. The ultimate load of SP1 is higher by 10%, SP2 is

higher by 7% compared to its monolithic counterpart, and RF1 is higher by 12%. The difference in yielding and ultimate behaviour of joint depends on the deformation in the joint components, such as deformations in bolts or embedded steel and endplate deformations. These deformations govern precast joints' yield and ultimate behaviour, whereas, in the monolithic joint, deformations in the reinforced concrete joint core governs the behaviour. Stress contours (Figure 13 and Figure 14) unveil the behaviour of precast joints SP1 and SP2, which are designed following strong column weak beam phenomena and capacity design considerations to avoid brittle shear failure. The stress contour plot PEMAG and PE (max, principle) indicate the specimen's plastic deformation and crack pattern. Critical stress location in rebar can also be observed from the plot. The plot concludes failure of both the joins are by beam flexure failure while the connection components remain elastic. Joint shear deformations are not observed throughout the analysis for both joints. The presence of an embedded plate in the joint region shifts the critical plastic zone away from the joint face. The FEM analysis conducted on both the joints reveal the elastic, yielding, and ultimate behaviour of the joint.

5.4. Connection rigidity

Depending on moment rotation characteristics, connections can be classified as rigid, semirigid or pinned. No connection is ideally rigid or pinned; all connections behave semirigid after flexural cracking. Elliott and Jolly (2013) introduced an approach called the beamline approach to measure the semi-rigidity of the connections. This approach is used to quantify the relation of moment–rotation and classify the connection. For an ideally rigid connection, a beam with a uniformly distributed load of w has a hogging moment MR = $WL^2/12$, the same beam, if it is pinned the end rotation, will be $\Theta = WL^3 / 24E_cI$. Hence the gradient of the beamline is $-2E_cI/L$. According to beamline theory, the connection can be considered rigid if the yield point ultimate point on moment-rotation plot lies above the beamline. Most importantly, the initial slope of the curve is almost vertical (close to 90°). According to beamline theory, the connections not satisfying the above criteria can be classified as semirigid or pinned Moment verses relative rotation graph of the specimen RF1, SP1 and SP2 obtained from FEM output and the corresponding beamline are plotted in Figure 15. In all the plots, the curve crosses the beamline, and the initial slope of the curve is nearly vertical. Hence the connections can be classified as rigid connections.

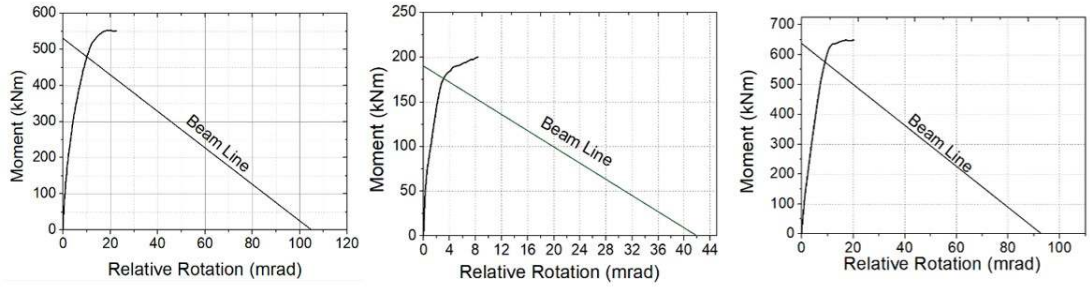

Figure 15. Stiffness of connection by beam line method

6. ANALYTICAL MODELLING AND CYCLIC RESPONSE OF THE JOINT

FEM analysis performed on the specimen provide parameters such as failure mode, force-displacement relations, ductility characteristics of the beam-column joints. Numerical analysis results were able to predict the strain hardening behaviour of the joint. But to obtain characteristics such as energy dissipation, equivalent viscous damping and stiffness degradation, it is required to simulate strain hardening and strain-softening behaviour of the joint. Numerical simulation of strain-softening behaviour of the joint is computationally expansive for nonlinear material like concrete. The post ultimate behaviour of the joint can be obtained by nonlinear analytical modelling of the joint in analytical software like SAP2000 by appropriately selecting the degradation parameters and material property. The beam-column joint can be modelled analytically by selecting appropriate elements (Girgin et al. 2017; French et al. 1989; Stone et al. 1995) and other nonlinear parameters as described. Beam and column elements can be modelled as elastic elements with lumped plasticity at the end region. Nonlinear deformations in the Joint panel zone can be modelled as a bi-linear spring element. But since the FEM result reveals no inelastic deformations in the joint region, nonlinear modelling of the joint panel zone is not required.

FEM analysis on the specimen reveals the failure is by the formation of beam flexure hinge. Hence properties of the beam flexure hinge govern the behaviour of the joint. The hinge property can be obtained by i. Section analysis or form ii. Moment-rotation plot obtained by FEM analysis. The section analysis method is ideally suitable for monolithic joint or the joint whose response characteristics are close to the monolithic response, whereas dry mechanical joints, whose response

characteristics vary from monolithic behaviour, the second method will be the most suitable for obtaining hinge properties. The moment-rotation response obtained for FEM analysis was idealised as a bi-linear curve as per the recommendations of ASCE/SCI standard 41-13 (2013) to obtain yield and ultimate point. Figure 16 provides the hinge definition parameters obtained for all the specimens. Hysteresis response and post ultimate behaviour of the joints. can be obtained analytically by appropriately selecting the hysteresis parameters and post ultimate behaviour of the material. "Pivot" hysteresis mode, a parameter-based model available in SAP2000, can accurately simulate the response. The governing parameters α and β of the "Pivot" model depend on the reinforcement ratio and axial load. A rectangular beam c/s with 1-1.5% reinforcement and negligible axial load, α = 6, β=0.6, can simulate the response with reasonable accuracy (Sharma et al., 2011). Hysteresis response ratio and axial load. obtained for the joint RF1, SP1 and SP2 were plotted in Figure 17. b to Figure 17.d. The plot obtained for specimen RF1 was compared with the experimental plot obtained by Aninthaneni et al. (2018). Except the variation at higher drift level due to post ultimate rebar buckling characteristic, which was not taken care of in the analytical simulation, the results of RF1 matched with the experimental results in general. This concludes that the analytical model on the beam-column joint can capture the joint's strain and softening characteristics.

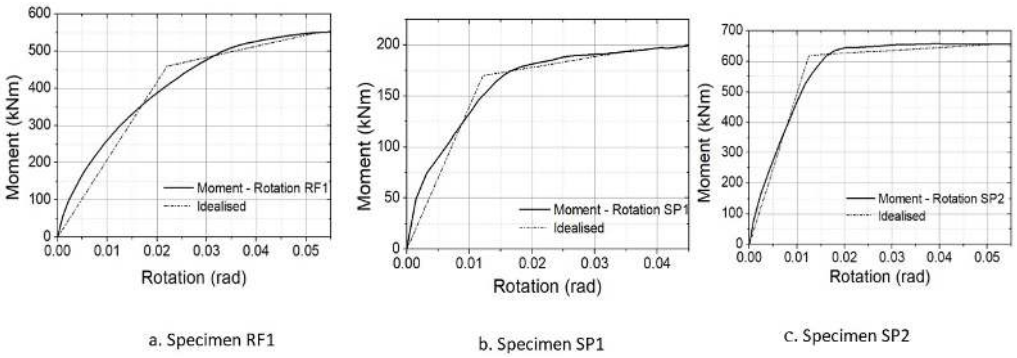

Figure 16. Moment – Rotation curve of the connections

Table 6. Yielding, Ultimate and ductility characteristics of the precast joints

Specimen	Yield Moment kNm	Yield Rotation rad	Yield Displacement mm	Ultimate Displacement mm	Ductility
RF1	460	0.0205	28	124	4.4
SP1	157	0.0121	15	68	4.5
SP2	620	0.012	36	154	4.2

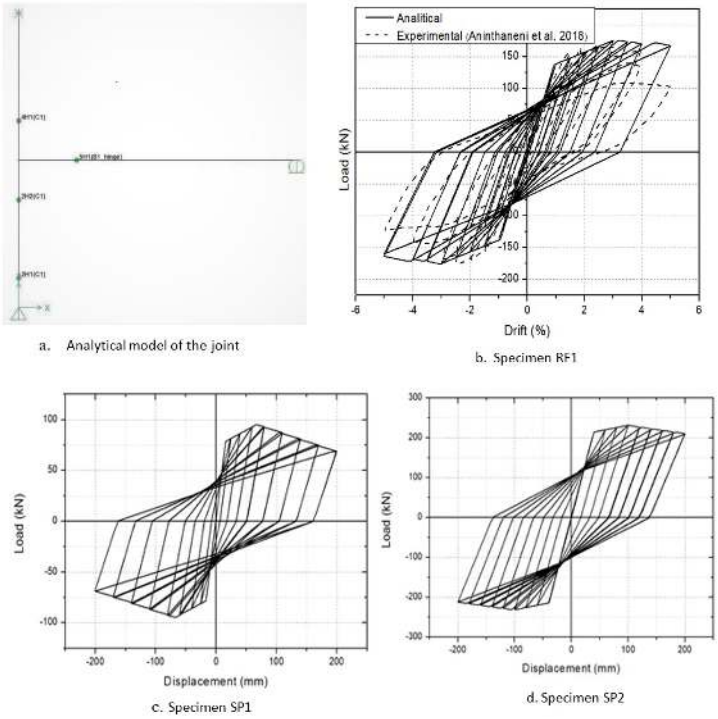

Figure 17. Analytical modelling of the precast joints and cyclic response of the joints

6.1. Ductility

Ductility is defined as the ability of the structure to undergo plastic deformations without significant loss of strength. Ductility is the desired element to ensure safety against catastrophic failure of structure in a severe seismic event. Ductility of beam-column joint, μ, is defined as the ratio of ultimate displacement to yield displacement of the joint. As described in the earlier section, yield displacement was determined based on the ASCE/SEI Standard 41-13 (2013) recommendations. The idealised bi- liner curve following the standard was in Figure 16. The ultimate deformation was considered as maximum deformation corresponding to the point on the moment rotation curve where there is no significant strength loss, and the maximum compressive strain in extreme compressive fibre is around 0. 0038. Table 6 provide the ductility of the specimens investigated. The force and corresponding displacements in the table were obtained from the force-displacement response of the analytical model (Figure 17 a), considering the nonlinear properties obtained from the idealised moment-rotation curve (Figure 16). The ductility of all the specimens obtained was more than 3.5. Hence the response can be classified as a fully ductile response (Paulty and Priestely 2013).

6.2. Stiffness degradation

The stiffness of the connection, which is the ratio of force to displacement, remains constant when the joint remains elastic; when the joint cross its yielding point, stiffness varies continuously with drift level. The line connecting the maximum force in any cycle and the origin represents the secant stiffness at that displacement cycle. The secant stiffness (Ks) was calculated as the ratio of the average of the peak positive and negative forces to the peak positive and negative displacements of the indented drift cycle. As the joint cross the yielding point, cracks start propagating, and plastic rotations take place at the critical region and stiffness offered by the joint will be reduced. Stiffness degradation can be observed from Figure 18a. for all three specimens. Stiffness degradation is steeper at 1% to 2.5% drift cycles. The stiffness of specimen SP1 is degrading at a higher rate when compared to RF1, whereas the rate of stiffness degradation of SP2 is comparable with RF1, whose response is close to the monolithic response. The stiffness of SP1 at 3.5% drift level is 0.15 x initial stiffness; hence all the specimens satisfy the requirements of ACI T 1.1 (2001).

6.3. Equivalent viscous damping

Energy dissipation and equivalent viscous damping are the essential characteristics to ensure the seismic performance of the connection. The energy dissipation capacity of the connection is equal to the area enclosed. by the hysteresis load-displacement loop, and equivalent viscous damping at any drift cycle is the ratio of energy dissipated during that particular cycle to the strain energy Inelastic deformations in structural elements and connections are the source for hysteretic damping in the structure. Hysteresis damping contributes a majority of the energy dissipated in the structure. A plot was made (Figure 18b) for equivalent viscous damping expressed as percentage versus displacement. From the plot, it is clear that energy dissipation and viscous damping are higher for the specimen SP1 when compared to the other two specimens, and the slope of SP1 curve is steeper at 1 – 2.5% drift level compared to the other two specimens. The performance of specimen SP2 Is comparable with the reference specimen, whose response was considered close to the monolithic response. Figure 18 reveals that specimen SP1 have better energy dissipation capacity than the other two specimens.

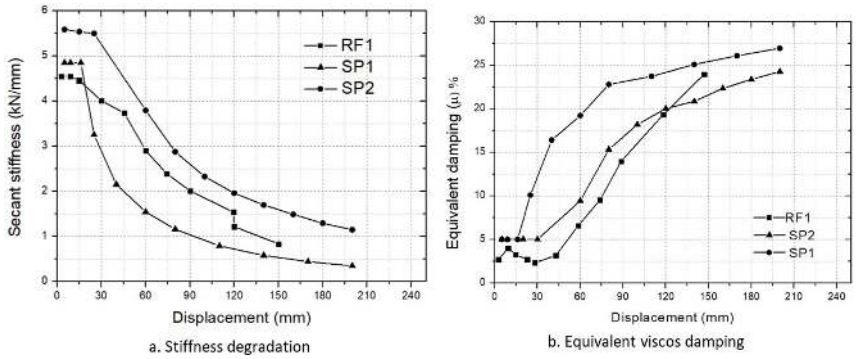

Figure 18. Response characteristics of the joints

7. CONCLUSIONS

Precast dry mechanical connection system consisting of endplate, stiffeners and bolts is faster to construct with less erection efforts. Many dry mechanical connection systems were studied in the past literature. The proposed joint consist of embedded bolts is easy to cast and erect with better load dispersion characteristics. The performance of the dry

connections was studied using finite elemental analysis. The proposed joints and their connection components were designed to ensure seismic performance. Three-dimensional nonlinear finite elemental analysis was performed on these designed joints to study the performance. The model of these joints was developed using solid elements in ABAQUS software. Reinforced concrete material properties and failure criteria were defined using the concrete damage plasticity model, and steel material properties were defined using von mises yielding criteria. The numerical model developed was validated with the experimental results.

The performance of precast joints designed following the capacity design criteria specified in the description section was verified using the validated FEM model. Below mentioned are the objectives achieved through this analysis

a. The adaptability of the capacity design considerations to the precast structures and the endplate connections designed following the equivalent yielding line length procedure was studied through this research.
b. The precast connection characteristics, when compared to monolithic connection was, investigated
c. The input required for simplified nonlinear analysis using any typical nonlinear analysis software was obtained from the numerical study performed.
d. The rigidity of the connection and initial elastic stiffness of the connection was obtained through this research

The following conclusions were drawn based on the finite elemental study of these joints.

1. Comparison of results of FEM analysis with the experimental results reveals that the numerical model, including the elements selected, interactions defined, and the material definition parameters, can predict the yielding and ultimate behaviour of the joint with reasonable accuracy.
2. The use of embedded bolts with annular plate will ensure better stress dispersion and optimise the number and diameter of bolts required.
3. The initial stiffness offered by precast joints designed is like the monolithic joint. Whereas the yield point and ultimate point is higher than that of the monolithic joints. Failure of precast joints is by beam flexure failure, while the connection components remain elastic. No shear deformations are observed in the joint region, which is desirable to ensure ductile behaviour.
4. The cyclic response, stiffness degradation and the energy dissipation plots obtained from the analytical model reveal that both the joints SP1 (designed for 5m span building) and SP2 (designed for 6m spam building) exhibit satisfactory stiffness and energy dissipation characteristics.
5. Depending on moment rotation characteristics, connections can be classified as rigid, semirigid or pinned; rigidity of connection can be measured based on the moment relative rotation relation of the joint. This relation varies depending on the strength and deformation characteristics of all the connection components. The moment relative rotation plots of the joints obtained from analysis were evaluated for semirigid behaviour based on the beamline method. The plots obtained concludes that the joints can be classified as rigid joints.
6. The moment rotation relation and the failure mode obtained from FEM analysis are inputs for analytical modelling of the joint. The results obtained from the analytical model of the joints predict the cyclic response and other essential characteristics with reasonable accuracy.
7. The numerical results will provide the input required for nonlinear modelling of the precast framed building using this beam-column connection. Hence, global nonlinear characteristics like energy dissipation, displacement profile, and seismic performance can be studied further.

Nomenclature

σ_c concrete compressive stress
σ_t concrete tensile stress
E_c modulus of elasticity of concrete
f_{ck} characteristics compressive strength of concrete
f_y/f_u steel yield stress/ultimate stress
f_t Tensile strength of concrete
ε_t , ε_c strain in concrete in tension and compression
$G(\sigma)$ non-associated plastic flow potential, Druker-Prager formulation
ψ dilation angle
$\bar{p}, \bar{q}$ the plane in which plastic potential function is defined
Kc ratio of second stress invariants on tensile and compressive meridians
$\varepsilon_c^{pl}/\varepsilon_t^{pl}/\varepsilon_c^{el}/\varepsilon_t^{el}/\varepsilon_c^{ch}/\varepsilon_t^{ck}/\varepsilon_{oc}^{el}/\varepsilon_{ot}^{el}$ strains (Figure 5); subindexes "c", "t", "oc" and "ot" and refer to compression, tension, undamaged compression and undamaged tension, respectively; super indexes "pl", "el", "ch" and "ck" and refer to plastic, elastic, crushing and cracking, respectively

$\frac{f_{bo}}{f_{co}}$ biaxial compressive yield strength/uniaxial compressive yield strength
dc concrete damage parameter in compression
dt concrete damage parameter in tension

Author's Contributions: Conceptualization, Srikanth K, Borghate S.B; Methodology, Srikanth K; Investigation, Srikanth K; Writing - original draft, Srikanth K; Writing – review, Borghate S.B; editing, Srikanth K; Supervision, Borghate S.B.

Editor: Marcílio Alves

8. References

ACI 318-02, (2002) Building code requirements for structural concrete and commentary. American Concrete Institute, Farmington Hills, MI, USA.

ACI T1.1-01, (2001) Acceptance criteria for moment resistance frames based on structural testing, American Concrete Institute, Farmington Hills, MI, USA.

ASCE/SEI 41-13, (2013) Seismic Evaluation and Retrofit of Existing Buildings, American Society of Civil Engineers, virginia.

Akanshu Sharma, Reddy, G.R., Vaze, K.K. (2011) Nonlinear seismic analysis of reinforced concrete framed structures considering joint distortion, Report No. BARC/2011/E/026, Bhabha atomic research centre, Mumbai, india.

Alfarah, B., López-Almansa, F., Oller, S. (2017). New methodology for calculating damage variables evolution in Plastic Damage Model for RC structures, Engineering Structures, 132, 70–86.

Alrazi Earij, Giulio Alfano, Katherine Cashell, Xiangming Zhou (2017). Nonlinear three–dimensional finite–element modelling of reinforced–concrete beams: Computational challenges and experimental validation, Engineering Failure Analysis, 82, 92–115.

Aninthaneni, P.K., Dhakal, R.P., Marshall, J., Bothara, J. (2018). Nonlinear Cyclic Behaviour of Precast Concrete Frame Sub-Assemblies with "Dry" End Plate Connection, Structures, 14, 124–136.

Bahrami, S., Madhkhan, M., Shirmohammadi, F., Nazemi, N. (2017). Behavior of two new moment resisting precast beam to column connections subjected to lateral loading, Engineering Structures, 132, 808–821.

BS EN 1993-1-8:2005, Eurocode 3: Design of steel structures - Part 1-8: Design of joints, European committee for standardisation, Rue de la Science 23. B-1040 Bruxelles, Belgium.

Choi, H., (2013). Development and testing of precast concrete beam-to-column connections, Eng. Struct., 56, 1820–35.

D'Arcy, T.J., Nasser, G.D., Ghosh, S.K. (2003). Building code provisions for precast/prestressed concrete: A brief history, PCI J., 48 (6), 116–124.

Elliot, K., Davies, G., Ferreira, M., Gorgun, H., Mahdi, A.A. (2003). Can precast Concrete structures be designed as semirigid frames? Part 1-The Experimental Evidence, Struct Eng., 81(16), 14–27.

Elliott, K. S., and Jolly, C.K. (2013). Multi-Storey Precast Concrete Framed Structures, 2nd edition. John Wiley, London.

French, C.W., Amu, O., Tarzikhan, C. (1989). Connections between precast elements failure outside connection region, J Struct Eng., 115 (2), 316–340.

Girgin, S.C., Misir, I.S., Kahraman, S. (2017). Seismic performance factors for precast buildings with hybrid beam-column connections. Procedia engineering, 199, 3540-3545.

Hawileh, R.A., Rahman, A., Tabataba, H. (2010). Nonlinear finite element analysis and modeling of a precast hybrid beam–column connection subjected to cyclic loads, Applied Mathematical Modelling, 34, 2562–2583.

Hossein Parastesh, Iman Hajirasouliha, Reza Ramezani (2014). A new ductile moment-resisting connection for precast concrete frames in seismic regions: An experimental investigation, Engineering Structures, 70, 144–157.

IS 13920-2016, Ductile detailing of reinforced concrete structures subjected to seismic forces. - code of practice., Bureau of indian standards, New Delhi.

IS 1893-2016, Criteria for earthquake design of structures, Bureau of indian standards, New Delhi.

Khaloo, A.R., Parastesh, H. (2003). Cyclic loading response of simple moment-resisting precast concrete beam-column connection, ACI Struct. J., 100(4).

Kulkarni, S.A., Li, B., Yip, W.K. (2008). Finite element analysis of precast hybrid-steel concrete connections under cyclic loading, J Constr Steel Res, 64 (2), 190-201.

Lubliner, J., Oliver, J., Oller, S., Onate, E. (1989). A plastic–damage model for concrete, Int. J. Solids Struct., 25 (3), 299–326.

Mohamed A., Shaheen, Konstantinos Daniel Tsavdaridis, Emad Salem (2017). Effect of grout properties on shear strength of column base connections: FEA and analytical approach, Engineering Structures, 152, 307–319.

Najafgholipour, M.A., Dehghan, S.M., Amin Dooshabi and Arsalan Niroomandi (2017). Finite element analysis of reinforced concrete beam-column connections with governing joint shear failure mode, Latin American Journal of Solids and Structures, 14, 1200-1225.

Najafgholipour, M. A., Arabi, A. R. (2019). A nonlinear model to apply beam-column joint shear failure in analysis of RC moment resisting frames, Structures 22, 13-27.

Nishiyama, M. (1990). Seismic design of prestressed concrete buildings, Bull. N. Z. Natl. Soc. Earthquake Eng., 23 (4), 288–304.

Nzabonimpa, J.D., Hong, W.K., Kim, J. (2017). Experimental and nonlinear numerical investigation of the novel detachable mechanical joints with laminated plates for composite precast beam-column joint, Composite Structures, 185, 286–303.

NZS 3101-1995, Concrete structures standard - The design of concrete structures, Standards New Zealand, Wellington.

Onur Ertas, Sevket Ozden, Turan Ozturan. (2006). Ductile connections in precast concrete moment resisting frames, PCI J., 51 (3), 66–76.

Otani, S. (1981). Hysteretic models of reinforced concrete for earthquake response analysis, Journal of Faculty of Engineering, University of Tokyo, 36 (2), 407-441.

Park, R.A. (1995). Perspective on the seismic design of precast concrete structures in New Zealand, PCI J., 40 (3), 40–60.

Paulina Krolo, Davor Grandic, Mladen Bulic (2016). The guidelines for modelling the preloading bolts in the structural connection using finite element methods, Journal of Computational Engineering.

Paulty, T., and Priestely M.J.N. (2013). Seismic Design of Reinforced Concrete and Masonry Buildings, Wiley, India.

Priestley, M., Sritharan, S., Conley, J., Pampanin, S. (1999). Preliminary results and conclusions from the PRESSS five-story precast concrete test building, PCI J., 44 (6), 42–67.

Rahman, M.A., Sritharan, S. (2007). Performance-based seismic evaluation of two five-story precast concrete hybrid frame buildings, Journal of structural engineering, 133 (11), 1489-1500.

Sofia Gavridou, John W Wallace, Takuya Nagae (2017). Shake-table test of a full-scale 4-story precast concrete building. I: overview and experimental results, Journal of Structural Engineering, 143-6, 04017034.

Stone, W.C., Cheok, G.S., Stanton, J.F (1995). Performance of hybrid moment-resisting precast beam–column concrete connections subjected to cyclic loading, ACI Struct J., 91 (2), 229–249.

Vidjeapriya, R., Jaya, K.P. (2013). Experimental study on simple mechanical precast beam-column connections under reverse cyclic loading, Journal of Perform. Constructed Facilities, 27 (4), 402-414.